

ShapeLib: Designing a library of programmatic 3D shape abstractions with Large Language Models

R. KENNY JONES, Brown University, USA

PAUL GUERRERO, Adobe Research, United Kingdom

NILOY J. MITRA, University College London and Adobe Research, United Kingdom

DANIEL RITCHIE, Brown University, USA

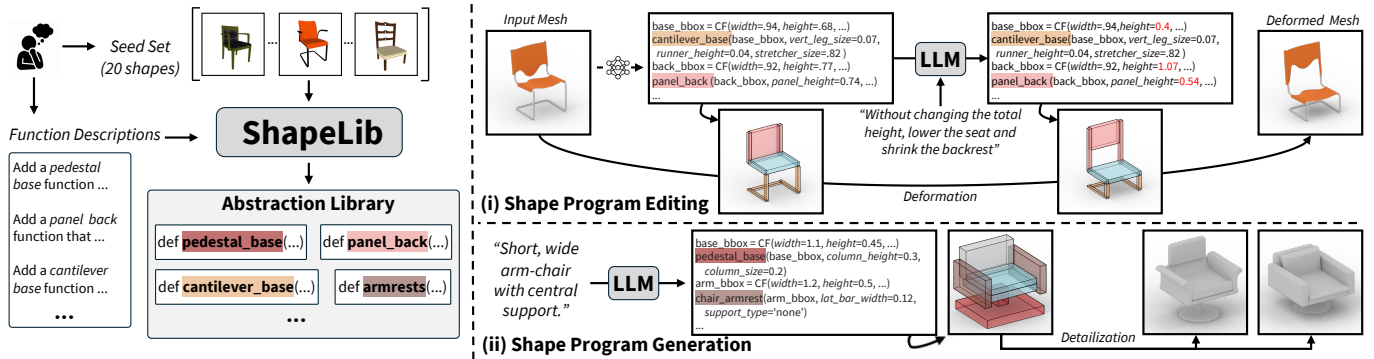


Fig. 1. ShapeLib guides an LLM to design a library of programmatic shape abstraction functions from a small set of seed shapes and function descriptions. These abstraction functions generalize beyond the seed set and expose semantically aligned, easy-to-work with interfaces, supporting downstream tasks like (i) shape editing (through LLM program editing and mesh deformation) and (ii) shape generation (through LLM program synthesis and detailization).

We present ShapeLib, the first method that uses LLM priors to design libraries of programmatic 3D shape abstractions. Our system accepts two forms of design intent: high-level text descriptions of functions to include in the output library and a small seed set of exemplar shapes. We discover a library that matches this design intent with a guided LLM workflow that first proposes different ways of applying and implementing abstraction functions, and then validates them. We also learn recognition networks that map shapes to programs that use these newly discovered abstractions by training on data produced by LLM-authored synthetic data generation procedures. Across multiple modeling domains (split by shape category), we find that LLMs, when thoughtfully combined with geometric reasoning, can be guided to author a library of abstraction functions that generalize to shapes outside of the seed sets. Our framework addresses the long-standing shape analysis problem of discovering reusable, programmatic shape abstractions while exposing interpretable, semantically aligned interfaces. We find that ShapeLib provides distinct advantages over prior alternative abstraction discovery works in terms of generalization, usability, and maintaining plausibility under manipulation. Finally, we demonstrate that ShapeLib’s abstraction functions unlock a number of downstream applications, combining LLM reasoning over shape programs with geometry processing tools to support shape editing and generation workflows.

CCS Concepts: • Computing methodologies → Shape modeling.

Additional Key Words and Phrases: shape analysis, shape abstraction, procedural modeling, large language models, library learning, interpretable

1 INTRODUCTION

3D shapes are central to many visual computing problems, where applications depend on the ability to edit, manipulate, analyze, and synthesize 3D assets. Procedural models—structured programs that produce geometry when executed—are an appealing representation for 3D shapes that provide natural support for these operations. Well-designed procedural models expose (semantic) handles that end-users can interpret and use to easily manipulate output geometry. Good programs, however, are expensive to author or acquire.

When experts design procedural models, they rely on libraries of modeling functions that expose the right level of abstraction for a particular domain. For instance, authoring a good procedural model of a building might require access to programmatic abstractions that tile windows over a facade [Wonka et al. 2003], or automatically extrude common types of roofing patterns from a boundary [Müller et al. 2006]. When interpretable modeling functions are not available, this shape modeling task becomes more difficult (see Figure 2).

Unfortunately, designing a library of procedural modeling functions is significantly more challenging than authoring a single procedural model. Despite this difficulty, researchers have investigated how to automatically discover libraries of programmatic abstractions [Ellis et al. 2021; Jones et al. 2023] with techniques that are unaware of shape semantics. Starting with a dataset of shapes and a base modeling language with elementary functions, these bottom-up methods greedily grow libraries by defining new functions based on how well they compress patterns over the dataset. While these methods successfully optimize their compression-based objectives, they develop their libraries without any semantic guidance, and as such the functions they produce only align to shape semantics by

Authors’ addresses: R. Kenny Jones, russell_jones@brown.edu, Brown University, USA; Paul Guerrero, guerrero@adobe.com, Adobe Research, United Kingdom; Niloy J. Mitra, n.mitra@cs.ucl.ac.uk, University College London and Adobe Research, United Kingdom; Daniel Ritchie, daniel_ritchie@brown.edu, Brown University, USA.

chance, making it difficult for users to understand or manipulate the resulting programmatic interface (see Figure 2).

As an alternative, we investigate how Large Language Models (LLMs) can help with this programmatic abstraction design problem. LLMs have demonstrated remarkable success over a surprisingly diverse range of tasks, from 3D layout synthesis [Hu et al. 2024] to general code generation [Jiang et al. 2024]. There are reasons to believe they might be useful in helping to design programmatic shape abstractions: they have world knowledge about the semantic relationships of parts within shapes and are proficient at writing code. At the same time, LLMs also have limitations that temper their usefulness for reasoning over programmatic shape representations. As we demonstrate experimentally, LLMs still struggle to understand complex geometric layouts and often misinterpret or misattribute constraints and relations between parametric controls.

To leverage LLMs, while avoiding these limitations, we propose ShapeLib, a hybrid system that guides an LLM through the creation of a library of programmatic shape abstraction functions from a specified design intent. A user provides this design intent in two forms: (i) high-level function descriptions in natural language, and (ii) a small seed set of exemplar shapes. The two modalities are complementary: the first mode allows the user to specify the kinds of functions they would like to interface with; while the second mode provides geometric references that guide and constrain library development. ShapeLib discovers functions that produce cuboid primitives that represent semantically aligned part bounding boxes. Instead of trying to completely reproduce surface geometry, we generate a structured shape representation that supports multiple downstream tasks (see Figure 1).

ShapeLib breaks the complex library design process into a series of sub-problems. First, we use an LLM to convert the user-provided function descriptions into a structured library interface. Next, we task an LLM with proposing a set of possible applications of these functions to explain shapes from the seed set. We then use these proposed applications to automatically formulate input/output examples that guide an LLM, in turn, to propose a set of possible function implementations. We finalize the library with a validation step that performs a geometric analysis over the proposed sets of possible function implementations and their applications. This pipeline ensures that the outputs of LLM-produced abstraction functions that get added into the library are grounded by patterns observed in the seed set.

To apply these functions to represent shapes outside of the seed set, we train *recognition networks* that learn to map input shapes to output programs that use the abstraction functions. To train this network, we task the LLM with creating a synthetic data generation procedure that uses the library functions to sample random programs that can be executed to form approximately correct part layouts. Thus, even starting from only a small seed set, ShapeLib can author programs that use these abstraction functions to explain a much larger collection of shapes.

We evaluate ShapeLib by using it to design libraries of programmatic abstraction functions over multiple shape modeling domains, which we split by category (chair, table, storage, lamp, faucet). Compared with alternative methods that discover shape abstractions, we experimentally demonstrate the benefits of ShapeLib’s

abstractions over a number of axes, including: (i) *Generalization*: abstractions are useful for modeling shapes outside of the seed set; (ii) *Usability*: abstractions expose an interpretable interface that is well-aligned with semantics, and hence easy to use; and (iii) *Plausibility*: abstractions constrain outputs to maintain shape semantics under manipulation.

ShapeLib relies on a novel blend of LLM guidance and geometric reasoning to outperform existing alternatives. Without semantic guidance, state-of-the-art geometry based systems like ShapeCoder [Jones et al. 2023] find abstractions that can generalize to new shapes, but are hard to interact with and produce non-semantic outputs under parameter modifications. Without a *seed set* of reference geometry, LLMs can convert *function descriptions* into seemingly sensible abstraction functions, but their implementations have structural inconsistencies which limits their ability to represent actual shape geometries. In contrast, ShapeLib exploits two complementary design intent modalities, guiding an LLM through the process of authoring programmatic shape abstractions, which prove useful in supporting downstream tasks, as depicted in Figure 1. For instance, we can perform shape edits by using our recognition network to infer a shape program, task an LLM to modify the program, and then modify the original geometry with a deformation. Alternatively, we can ask an LLM to convert a text prompt into a shape program, and then convert this structured representation into detailed geometry.

In summary, our contributions are:

- (1) ShapeLib, the first approach that, given a seed set and textual function descriptions as input, guides an LLM through the development of a library of programmatic shape abstraction functions that are reusable and semantically aligned.
- (2) Recognition networks that learn from LLM-authored synthetic data samplers to infer programs using the discovered functions.
- (3) Demonstrations of how programmatic shape abstraction support downstream applications like shape editing and generation.

2 RELATED WORK

Library Learning. The goal of library learning is to automatically discover a set of useful programmatic abstractions. Several prior works [Cao et al. 2023; Ellis et al. 2018, 2021] have studied this task for general program synthesis domains. These methods take as input a set of simple tasks or programs that use only basic operators and find a library of more abstract functions that can represent the inputs more compactly. Though these approaches have demonstrated impressive generality, their non-specialization has limited their usability for more complex 3D modeling domains. ShapeMOD [Jones et al. 2021] and ShapeCoder [Jones et al. 2023] extend this library learning machinery to 3D shapes, using specialized search strategies over parametric expressions. However, unlike ShapeLib’s use of an LLM prior, all of the above methods derive the library based *only* on the input examples. As we find experimentally, this limits the *interpretability* of the functions discovered by these methods, which produce interfaces that are hard to work with and align poorly with semantics. Lilo [Grand et al. 2024] is a recent approach that also leverages an LLM prior for general library learning. However, in Lilo, the LLM is only used to *name* functions found by a non-semantic

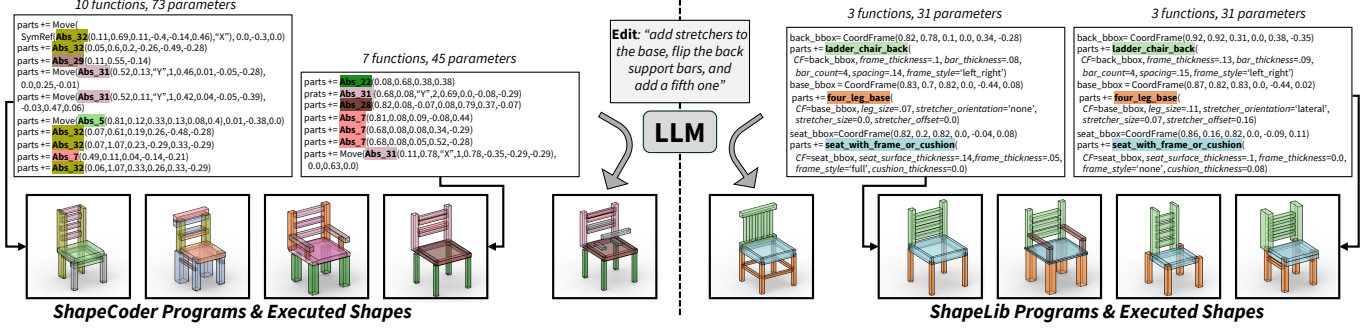


Fig. 2. Comparing programs found when using different library learning methods to represent the same set of shapes. ShapeCoder [Jones et al. 2023] (left) discovers abstractions without semantic guidance, which is ill-suited for downstream tasks like shape editing (middle). ShapeLib (right) exposes an easy to understand interface, with semantically named parameters, and applies functions in a consistent fashion.

compression-based method [Bowers et al. 2023], so the prior issues still remain.

Shape Program Synthesis. A number of learning-based methods have studied the shape program synthesis problem for specific low-level languages, such as CSG modeling [Kania et al. 2020; Ren et al. 2021], CAD workflows [Willis et al. 2020; Wu et al. 2021], L-systems [Guo et al. 2020; Lee et al. 2023]. Other approaches have investigated how to extend this machinery to work over more general visual programming domains [Ganeshan et al. 2023; Jones et al. 2024; Sharma et al. 2018]. While these methods assume that the domain-specific languages are fixed and known ahead of time, ShapeLib aims to discover a library of new abstraction functions directly.

The visual programs we consider represent complex shapes through a combination of simple part primitives; many inverse modeling works have taken a similar framing [Hu et al. 2023; Jones et al. 2020; Li et al. 2017; Mo et al. 2019a]. Unlike these prior works, ShapeLib leverages an LLM to create compact, semantic programmatic interfaces for these structured representations. Prior work has found that shape programs that use only general, low-level operations hurt performance on downstream tasks and expose interfaces that users find more difficult to manipulate [Jones et al. 2021]. A possible solution is first to have an expert user author complex procedural models capable of representing large shape families and then to train networks that learn how to parameterize these programs [Pearl et al. 2022; Raistrick et al. 2023, 2024]. This approach can produce compelling results, but it is expensive and time-consuming to ask an expert to craft well-designed procedural functions. In contrast, ShapeLib explores how an LLM can be guided through the process of automatically designing useful abstraction functions from easily provided, high-level design intent.

LLMs for 3D Generation and Editing. LLMs have recently been used to directly generate scene layouts from natural language prompts [Aguina-Kang et al. 2024; Feng et al. 2023; Littlefair et al. 2025; Tam et al. 2024; Yang et al. 2024; Zhang et al. 2024]. These methods take an opposite approach to those in the prior paragraph: they rely almost wholly on the LLM prior, and only extract limited information from the seed set (e.g., as in-context examples). Though similar at surface level, shape modeling and scene modeling present different difficulties, as part-to-part relations in shapes have more constrained and specific relationships than object-to-object

relations in most scenes. We experimentally find that ablated versions of ShapeLib that minimize reliance on the prior provided by seed set perform significantly worse. Relatedly, some recent work has explored how LLMs might enable visual editing workflows. ParSEL [Ganeshan et al. 2024] uses an LLM to convert a structured shape representation into an approximate procedural model that supports a particular user-specified edit. BlenderAlchemy [Huang et al. 2024] uses an LLM to modify existing procedural shapes and scenes encoded as blender programs. 3D-GPT [Sun et al. 2023] uses an expert-designed library of procedural modeling functions [Raistrick et al. 2023] to synthesize and edit virtual worlds. However, these prior approaches require highly structured inputs, such as expert-designed procedural models. In contrast, we study how to automatically discover useful programmatic shape abstractions, which we can then use to edit unstructured input shapes.

3 DESIGNING A LIBRARY OF SHAPE ABSTRACTIONS

ShapeLib guides an LLM through the process of developing a library of programmatic abstraction functions from an input design intent. In our framing, we assume that a user has a shape modeling domain in mind (e.g., a shape category), and communicates this design intent to our system with two modalities: function descriptions and a seed set of shapes. Describing desired function properties helps to constrain the design of the interface, attuning the LLM towards a particular way of solving the modeling task. Each seed set we consider is composed of 20 shapes with part-level semantic segmentations and textured renders. ShapeLib finds programmatic representations of these shape structures, with functions that output part bounding proxies. In this way, our programmatic abstractions also provide a layer of geometric abstraction.

ShapeLib’s framing receives a number of benefits from the prior knowledge encoded in LLMs. As LLMs have been trained extensively on human-written code, they are able to author functions with meaningful names and parameters. This exposes an interface that is semantically aligned, and easy to work with. However, LLMs, by themselves, are prone to hallucinate, generating mismatches from ‘real’ distributions of shapes. To overcome this limitation, our system validates the plausibility of its productions by searching for function implementations and applications that can explain sub-structures in the seed set shapes. Figure 3 shows our overall

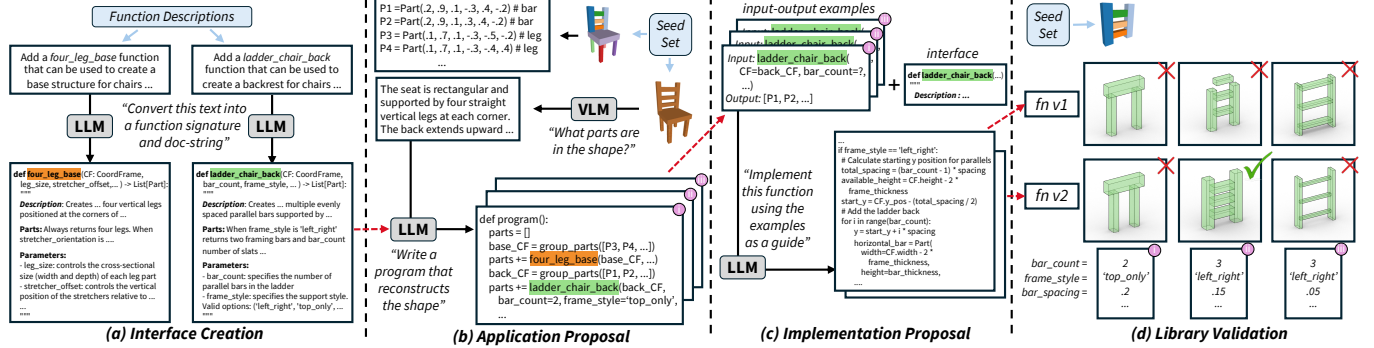


Fig. 3. ShapeLib overview. We design a function library in four steps, starting from function descriptions and a set of seed shapes. First, (a) we prompt an LLM to create function interfaces that define parameters and annotate the function’s purpose. Then, (b) the LLM is prompted to propose multiple applications of the functions that reconstruct the seed shapes. Next, (c) we use this information to guide the LLM to propose multiple function implementations (Sec. 3.3). (d) library validation finalizes the library through geometric analysis (Sec. 3.4).

pipeline, which is divided into four stages: (a) *interface creation* converts function descriptions into a library interface (Sec. 3.1); (b) *application proposal* identifies which library functions should model which seed set shapes (Sec. 3.2); (c) *implementation proposal* generates candidate function implementations (Sec. 3.3); (d) *library validation* finalizes the library through geometric analysis (Sec. 3.4).

3.1 Interface Creation

ShapeLib first converts user function descriptions into a library interface (Fig. 3, a). We prompt an LLM to produce a structured interface, where for each function it produces a typed signature and an accompanying doc-string. We provide the LLM with two default classes: a *Part* class defines axis-aligned cuboid primitives that abstract detailed geometry and a *CoordFrame* class defines a local bounding volume. The LLM produces function signatures that expose parametric handles, e.g., the numbers of bars in a ladder back or the height of a base runner. Each function is instructed to take in a special first parameter, *CF*, a *CoordFrame* that specifies the expected extents of the functions outputs. Functions are typed so that they return a list of *Part* objects.

Through in-context examples and instructions, we prompt the LLM designed doc-string to have a particular structure. First, it defines a *description* field to explain the high-level goals of the function. Then, it defines a *parts* field, that specifies what kinds and how many parts should be produced depending on the input parameters. Finally, it defines a *parameter* field, that explains how each variable should affect the output structure. This interface is then used in subsequent stages to guide the library development.

3.2 Application Proposal

As LLMs are prone to hallucinate, we do not directly implement functions following the prior step. Instead, we would like to be able to ground each function implementation by making sure it is capable of reproducing some structures from the seed set. To this end, we first propose programs that apply only library functions to explain the exemplar shapes (Fig. 3, b).

We begin by sampling a shape from the seed set and ask an LLM with vision capabilities (i.e., a VLM) to describe the parts that it

sees when given a rendering of the shape. We also convert the 3D semantic part annotations into a list of labeled *Part* objects. We combine these inputs together, and task an LLM with writing a program that uses the library functions to recreate the list of *Parts*. As we have not created function implementations yet, the LLM chooses functions and their parameters based only on the interfaces defined previously. We ask the LLM to use a special *group_parts* function when constructing this program, that consumes a list of input *Part* objects and returns a bounding *CoordFrame* object. With this formulation, we can automatically parse input-output examples; i.e. input parameters and the corresponding parts the functions should generate.

As we later demonstrate empirically, the accuracy of individual LLM calls has a high variance, which makes them hard to trust. Therefore, instead of finding a single program for each shape, we run this procedure K_A times for each shape in the seed set ($K_A=5$).

3.3 Implementation Proposal

ShapeLib now has the information it needs to author good function implementations: typed signatures, doc-string guidance, and input-output examples. From this input, we ask the LLM to complete the implementation of each function so that it matches the signature type, meets the doc-string specification, and respects the observed patterns present in the usage examples (Fig. 3, c). Of note, we find that the LLM predictions in the application proposal step do a good job of identifying which functions should explain which parts, but are less proficient at predicting reasonable parameter values. With this in mind, we mask out parameter values with a special token (?) when formulating input-output examples for the implementation prompt. We do this for every parameter value, except for *CF*, as the correct input value for this parameter, with respect to a specific set of outputs *Parts*, can be found automatically with the *group_parts* function.

Similar to before, we find that implementations authored by the LLM display substantial variance in terms of how well they match the input specification. So, for each function in our library, we propose K_I different ways that it could be implemented ($K_I=4$).

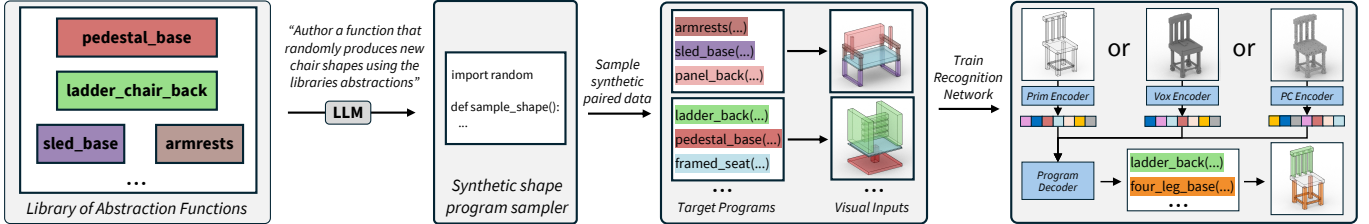


Fig. 4. To extend library usage beyond the seed shapes, we guide the LLM to author a synthetic data generator that uses the library functions. We then sample this function to produce paired synthetic data that can be used to train a recognition network that learns how to map shapes to programs.

3.4 Library Validation

From the prior steps we have (a) function doc-strings and signatures, (b) input-output usage examples, and (c) proposals of how the function should be implemented. The validation step is responsible for deciding which of these proposals are *grounded* (e.g., observed in the seed set) and not just LLM hallucinations (Fig 3, d).

To make this decision, for each function, we gather all of the LLM generated input-output examples, and separate them into a list of input parameter sets, and a list of output part sets. We use the former list to come up with a much larger set of ways that the function could be parameterized. Then, we execute the function on all parameter combinations from this set, and for each input set, we check if the functions execution matches any of the output part sets. We calculate this match with an error metric that compares corner-to-corner distances between sets of geometric primitives, and mark function applications as invalid if the paired structures incur an error that surpasses a threshold. Compared with the alternative of only checking the paired LLM input-output predictions, we observed this simple search strategy was able to successfully recover from LLM mistakes in this difficult reconstruction task.

At this point, for each group of parts from (b) we record which implementation from (c) best matches the observed part structure. We keep the implementation that achieves the *best* error across the *most* part groups, and remove all others proposals. If this *best* implementation found valid applications across multiple seed set shapes, we update the library interface entry with its implementation logic. Otherwise, we remove the function entry from the interface.

4 A LIBRARY SPECIFIC RECOGNITION NETWORK

In Section 3, we constructed a library of shape abstraction functions that capture patterns observed in the seed set, but a question remains: how can we use these functions to represent new shapes? In this section, we describe our strategy for expanding library function usage beyond the seed set with a recognition network, depicted in Figure 4. This network learns how to solve an inverse task: given an input shape, it reconstructs the shape by writing a program that uses the abstraction functions. We train our recognition network in a supervised fashion, using paired synthetic data generated by an LLM authored procedure. We first describe the generation of this synthetic data sampler, and then describe the design of our recognition network.

Generating a Synthetic Shape Program Sampler. In this step, we once again make use of the strong prior of LLMs by asking it to design a procedure that uses the abstraction functions to randomly

synthesize synthetic shape programs. To accomplish this, we design a prompt that describes the library we have developed, including the interface of each function and examples of how to use the abstractions (sourced from the validation stage). This prompt asks the LLM to design a *sample_shape* function that randomly produces new shape programs using the provided abstractions. Interestingly, we find that frontier LLMs are able to provide useful implementations of such a *sample_shape* function. As shown in Figure 4, some of these random outputs produce good shape abstractions, while other random samples violate class semantics. With this in mind, instead of attempting to get the LLM to perfect its implementation, we treat its output as a synthetic data generator for our recognition network. To broaden the coverage and variety of structures that these *sample_shape* functions produce, we employ an iterative refinement loop that provides automatic feedback to the LLM. This procedure ensures that all functions and parameters in the library get used, encouraging the *sample_shape* function to produce outputs spanning the observed structures from the validation step.

Training a Recognition Network. We implement our recognition networks as autoregressive Transformer decoders [Vaswani et al. 2017]. These networks use a causal prefix mask to attend to tokens produced by an encoder that consumes an input shape. They output a program, using the library functions, as a sequence of discrete tokens. This paradigm supports different visual input modalities by changing the kind of encoder: e.g., a shape represented as a collection of unordered primitives can treat discretized primitive parameters as tokens, while a shape represented as a voxel grid can be encoded with a 3D-CNN. We use the *sample_shape* function to create paired (visual input, program) data, which we use to train the recognition network with supervised updates (cross-entropy loss on program tokens). Specifically, we sample a random shape program using the LLM designed procedure, execute the program to produce a collection of primitives, and optionally convert these primitives into unstructured geometry (voxelization or surface point sampling). As the *sample_shape* functions use randomized calls, they produce an unlimited amount of paired data, so we train in a ‘streaming’ fashion by creating paired data on the fly.

5 RESULTS

We evaluate ShapeLib with experiments over multiple shape modeling domains, split by category: chair, table, storage, lamp, faucet. For each category, design intent is provided as high-level descriptions of functions that would be useful for this category and as a set of 20 seed shapes sourced from PartNet [Mo et al. 2019b].

Table 1. Comparing library learning implementations along the following axes: function usage, semantic consistency, and reconstruction (see Section 5.1)

Method	Fn Usage			Semantics			Reconstruction	
	# Fns per Shape ↓	# Fns per Lib ↓	Prog Dof ↓	Precision ↑	Recall ↑	F1 score ↑	F-Score (PC) ↑	IoU (Voxel) ↑
LLM-Only	14.9	5.6	63.5	34	12	18	37.4	34.9
ShapeCoder	13.5	19.2	48.6	25	30	27	40.9	32.3
ShapeLib	9.6	5.6	47.8	50	30	36	54.0	50.0

This input is provided to ShapeLib, which then produces libraries of abstraction functions for each category. Unless otherwise noted, we use OpenAI’s o1-mini as the LLM and gpt-4o as the VLM.

We compare ShapeLib against alternative abstraction discovery methods. (i) *LLM-Only* is an ablated version of our approach that ignores the seed set, asking the LLM to implement the library from the function descriptions alone. (ii) *ShapeCoder* [Jones et al. 2023] is a state-of-the-art system that relies on purely geometric reasoning, without semantic guidance (from any LLM). In Section 5.1, we evaluate how well libraries produced by these different methods are able to represent validation shapes. We then demonstrate that abstractions produced by ShapeLib are better suited for downstream tasks, like shape editing (Sec. 5.2) and shape generation (Sec. 5.3). Lastly, we validate the design of ShapeLib with a series of ablation studies (Sec. 5.4).

5.1 Evaluating Shape Abstraction Libraries

Library and Function Usage. To measure how well discovered libraries generalize beyond the seed set, we use recognition networks to infer shape programs that explain validation shapes from PartNet. First, we consider the case where each shape is represented as a collection of unordered primitives. For this reconstruction task (Table 1), we track how many function calls were needed to reconstruct each shape (*#Fns per Shape*) and how many degrees of freedom are exposed in the inferred shape programs (*Prog Dof*). We also report how many functions are included in each library (*#Fns per Lib*). From these results, we observe that ShapeLib offers distinct advantages over both LLM-Only and ShapeCoder. It uses fewer function calls per each inferred shape programs, exposing a simpler interface. Compared with LLM-Only, we find programs that successfully apply abstraction more often, leading to improved *Prog Dof* values. Compared with ShapeCoder, we discover significantly more compact libraries, avoiding function bloat.

Semantic Alignment. We show examples of inferred programs from validation shapes represented with primitives in Figure 2. Compared with ShapeCoder’s predictions (left), ShapeLib’s predictions (right) provide a programmatic interface that is easier to understand, as each function and parameter has a semantically relevant name. Beyond this, ShapeCoder uses multiple abstractions to represent the same type of structure in different reconstructions, which is undesirable. In contrast, ShapeLib’s functions are applied in a consistent fashion across the entire shape collection.

We quantitatively compare the semantic alignment of these different libraries by using them to perform semantic segmentation. For each function, we look at the applications made over the seed set, and record the semantic labels of parts that each function explains. We then aggregate this information by counting the most commonly covered part labels to produce a simple voting function,

which assigns semantic labels when the function is applied. We evaluate the semantic segmentation performance on fine-grained part labels from PartNet over validation shapes, and report results in the *Semantics* columns of Table 1. ShapeCoder and ShapeLib achieve a similar recall, but ShapeLib is twice as precise in its semantic predictions. LLM-Only is more precise than ShapeCoder; however, without access to seed set exemplars, it cannot find many successful function application, resulting in poor recall.

Reconstructing Unstructured Geometry. So far, we used structured recognition networks that consume shapes represented as primitive soups, but what about unstructured geometry? As discussed in Section 4, we can use recognition networks that replace a primitive encoder with either a point cloud or a voxel encoder. We report results for this experiment in the *Reconstruction* rows of Table 1. For the point cloud to program task, we sample a point cloud from the abstracted cuboid outputs, and report the F-score [Knapitsch et al. 2017]. For the voxel to program task, we convert the program’s execution into a voxel field, and report IoU. We find that ShapeLib infers more accurate reconstructions from these unstructured inputs, compared with ShapeCoder or LLM-Only. We visualize some qualitative comparisons of this experiment in Figure 6 (c). Beyond more faithful reconstructions, again we observe that ShapeLib’s function applications are more semantically correlated.

5.2 Editing Shape Programs

Editing with LLMs. A good library of programmatic abstractions should expose an interface that is easy-to-use and maintains shape plausibility under manipulation. We evaluate these properties by comparing how well an agent (i.e., an LLM) can edit shape programs in a goal-directed fashion. With libraries produced by either ShapeLib or ShapeCoder, we first use recognition networks to find shape programs that reconstruct validation shapes. Then, after designing a series of shape edit requests in natural language, we can ask an LLM to edit the text of the shape program to meet the request (i.e., change function parameters and how functions are used, as depicted in Figure 1).

We provided *o1mini* with the fully implemented function library for both ShapeLib and ShapeCoder conditions. To evaluate performance, we designed a two alternative forced choice perceptual study. We recruited 13 participants, who made 25 judgments each, over 100 possible shape edit comparisons. We asked each participant to make two judgments: (i) which manipulated shape was more plausible; and (ii) which edit better matched the input edit request. The results of this perceptual study (Table 2) provide further support of ShapeLib advantages. Our library of shape abstraction functions provides an easy-to-use interface, leading to edits that more often match the edit intent, while at the same time maintaining better shape plausibility under parameter variations. We show qualitative

Table 2. Results of our perceptual study evaluating edits made by an LLM to programs that use shape abstraction libraries. We report judgments along two axes: shape plausibility and match to edit intent.

More Plausible(%)	Better Matches Intent (%)
vs. ShapeCoder	75%

demonstrations of these edits in Figure 6 (a), and observe higher semantic alignment of LLM edits using ShapeLib programs.

Deforming Geometry with Program Edits. LLMs can successfully edit abstracted shape representations through program modifications, but what about edits to detailed geometry? We show examples in Figure 6 (b) of how ShapeLib can support text-driven mesh edits. In this proposed workflow, a mesh is first converted into a point cloud, which we pass into our recognition networks to find a reconstructing program. Then, we ask an LLM to modify this shape program with respect to an input edit request. We can then apply a simple cage deformation on the mesh vertices by treating the output parts of the original program as the initial cage, and the output parts of the edited program as the edited cage. As shown in Figure 6 (b), this workflow is able to produce compelling shape edits by leveraging the benefits of ShapeLib.

5.3 Shape Generation

Shape Program Generation. Beyond shape editing, we explore how ShapeLib can benefit generation tasks. To generate new structured shape representations, we can synthesize new shape programs, but who will author them? We design an experiment that uses LLMs to convert text descriptions into shape programs. We provide an LLM with a library of shape abstractions functions, and in-context examples of how text descriptions map to shape programs, sourced from the seed set. Then, given a new text description, we can ask the LLM to author a new shape program. Given a starting set of 10 shape descriptions, we prompt a LLM through ideating 50 new descriptions, designed to span common structural variations across a category. With this set, we compare ShapeLib against ShapeCoder and LLM-Only, generating 2 shape programs per description (producing 500 shape programs per method in total).

We report results of this experiment in Table 3. We can evaluate the distributional similarity of the LLM generated structures against structures from PartNet validation shapes, which act as a reference set. For Frechet PointNet++ Distance (*FPD*) and Kernel PointNet++ Distance (*KPD*) we use a feature space of a pretrained ShapeNet classification network. Minimum matching distance (*MMD*) reports the average minimum Chamfer distance of each member of the reference set to any member of the generated set. We also show qualitative examples of this text-to-program generation task in Figure 6 (d). Overall, we find that LLMs generate better shape structures when using ShapeLib libraries, as our semantically aligned abstraction expose an easy-to-use programmatic interface.

Structure Conditioned Detailization. What if we want to convert these abstracted shape structures into more detailed geometry? For this task, we use a structure-conditioned detailization module that consumes a set of primitives and outputs a mesh with geometric details, as shown in Figure 1. While a few existing systems have been designed for this purpose, they do not scale as well to the

Table 3. LLM shape program generation experiment, measuring distributional similarity against validation structures (averaged over each category).

Method	FPD ↓	KPD ↓	MMD ↓
LLM-Only	2219	717	0.100
ShapeCoder	449	31	0.091
ShapeLib	278	26	0.079

structurally complex primitive layouts produced by ShapeLib programs. Therefore, we propose a lightweight alternative where we adapt a recent state-of-the-art 3D generative model [Roblox 2025] to condition its predictions on an input set of primitives, through finetuning on PartNet. We find that this simple approach performs quite well. As shown in Figure 6 (e), we can convert structured ShapeLib programs into meshes with interesting geometric details that largely respect the input layout.

5.4 ShapeLib Ablation Experiments

We validate our design decisions with a series of ablation experiments, and find that our choices prove important to the success we observed in the previous sections; we refer readers to the appendix for full details and results. Below, we discuss the results of two ablation conditions of particular note.

ShapeLib Variants. By default the ShapeLib condition uses o1mini as its LLM. We investigated how library learning performance changes when this LLM is replaced with other frontier LLM models. We observed that when the *seed set* is absent, none of the LLM variants were able to match the performance of ShapeLib.

Seed Set Variants. ShapeLib is designed to operate over harmonious system inputs provided by a user: ideally, the shapes in the seed set should match the concepts listed in the function descriptions. What happens when these design intents are less tightly coupled? As an extreme, what if the seed sets are selected randomly from a large shape collection? While we find ShapeLib performs best with user-picked seed sets, these reformulations still outperform existing systems, while reducing the required effort on the part of the system user.

6 CONCLUSION

We have presented ShapeLib as the first method that uses LLM priors to produce a library of programmatic 3D shape abstractions that *generalize* over shape collections, expose *interpretable* parameters, and maintain *plausible* outputs under manipulation. We make use of two forms of complementary design intent, a seed set of example shapes and descriptions of functions to include in the library, to create shape programs that are compact and semantically well-aligned, supporting downstream applications like reconstruction, editing, and generation. Looking forward, this framing unlocks a number of exciting future opportunities. For instance, one could extend beyond single-category libraries toward a more general ‘meta-category’ framing, where a shared function library supports a diverse, but related set of categories. Another promising direction might use the LLM as a hypothesis generator for function descriptions, which would then need to be validated, perhaps by including the user ‘in-the-loop’. Finally, continued iteration on structured detailization

modules would be important to improve the coupling between high-level structure and geometric output. If this can be achieved while explicitly disentangling ‘style’, it would help bring us closer towards fully automatic, high-quality procedural model creation.

REFERENCES

Rio Aguina-Kang, Maxim Gumin, Do Heon Han, Stewart Morris, Seung Jean Yoo, Aditya Ganeshan, R. Kenny Jones, Qihong Anna Wei, Kailiang Fu, and Daniel Ritchie. 2024. Open-Universe Indoor Scene Generation using LLM Program Synthesis and Uncurated Object Databases. *arXiv preprint arXiv:2403.09675* (2024).

Matthew Bowers, Theo X. Olaussou, Lionel Wong, Gabriel Grand, Joshua B. Tenenbaum, Kevin Ellis, and Armando Solar-Lezama. 2023. Top-Down Synthesis for Library Learning. *Proc. ACM Program. Lang.* 7, POPL, Article 41 (jan 2023), 32 pages. <https://doi.org/10.1145/3571234>

David Cao, Rose Kunkel, Chandrakana Nandi, Max Willsey, Zachary Tatlock, and Nadia Polikarpova. 2023. Babbie: Learning Better Abstractions with E-Graphs and Anti-Unification. *Proc. ACM Program. Lang.* 7, POPL, Article 14 (jan 2023), 29 pages. <https://doi.org/10.1145/3571207>

Kevin Ellis, Lucas Morales, Mathias Sablé-Meyer, Armando Solar-Lezama, and Joshua B. Tenenbaum. 2018. Library Learning for Neurally-Guided Bayesian Program Induction. In *Advances in Neural Information Processing Systems (NeurIPS)*.

Kevin Ellis, Catherine Wong, Maxwell Nye, Mathias Sablé-Meyer, Lucas Morales, Luke Hewitt, Luc Cary, Armando Solar-Lezama, and Joshua B. Tenenbaum. 2021. Dreamcoder: Bootstrapping inductive program synthesis with wake-sleep library learning. In *Proceedings of the 42nd ACM SIGPLAN international conference on programming language design and implementation*. 835–850.

Weixi Feng, Wanrong Zhu, Tsu-jiu Fu, Varun Jampani, Arjun Akula, Xuehai He, Sugato Basu, Xin Erli Wang, and William Yang Wang. 2023. LayoutGPT: Compositional Visual Planning and Generation with Large Language Models. *arXiv preprint arXiv:2305.15393* (2023).

Aditya Ganeshan, Ryan Huang, Xianghao Xu, R. Kenny Jones, and Daniel Ritchie. 2024. ParSEL: Parameterized shape editing with language. *ACM Transactions on Graphics (TOG)* 43, 6 (2024), 1–14.

Aditya Ganeshan, R. Kenny Jones, and Daniel Ritchie. 2023. Improving unsupervised visual program inference with code rewriting families. In *Proceedings of the IEEE/CVF International Conference on Computer Vision*. 15791–15801.

Gabriel Grand, Lionel Wong, Maddy Bowers, Theo X Olaussou, Muxin Liu, Joshua B Tenenbaum, and Jacob Andreas. 2024. Lilo: Learning interpretable libraries by compressing and documenting code. *ICLR* (2024).

Jianwei Guo, Haiyong Jiang, Bedrich Benes, Oliver Deussen, Xiaopeng Zhang, Dani Lischinski, and Hui Huang. 2020. Inverse procedural modeling of branching structures by inferring L-systems. *ACM Transactions on Graphics (TOG)* 39, 5 (2020), 1–13.

Wentao Hu, Jia Zheng, Zixin Zhang, Xiaojun Yuan, Jian Yin, and Zihan Zhou. 2023. PlankAssembly: Robust 3D Reconstruction from Three Orthographic Views with Learnt Shape Programs. In *ICCV*.

Ziniu Hu, Ahmet Iscen, Aashi Jain, Thomas Kipf, Yisong Yue, David A Ross, Cordelia Schmid, and Alireza Fathi. 2024. SceneCraft: An LLM Agent for Synthesizing 3D Scenes as Blender Code. In *Forty-first International Conference on Machine Learning*.

Ian Huang, Guandao Yang, and Leonidas Guibas. 2024. Blenderalchemy: Editing 3d graphics with vision-language models. In *European Conference on Computer Vision*. Springer, 297–314.

Juyong Jiang, Fan Wang, Jiasi Shen, Sungju Kim, and Sunghun Kim. 2024. A Survey on Large Language Models for Code Generation. *arXiv preprint arXiv:2406.00515* (2024).

R. Kenny Jones, Theresa Barton, Xianghao Xu, Kai Wang, Ellen Jiang, Paul Guerrero, Niloy J. Mitra, and Daniel Ritchie. 2020. ShapeAssembly: Learning to Generate Programs for 3D Shape Structure Synthesis. *ACM Transactions on Graphics (TOG)*, *Siggraph Asia 2020* 39, 6 (2020), Article 234.

R. Kenny Jones, David Charatan, Paul Guerrero, Niloy J. Mitra, and Daniel Ritchie. 2021. ShapeMOD: Macro Operation Discovery for 3D Shape Programs. *ACM Transactions on Graphics (TOG)*, *Siggraph 2021* 40, 4 (2021), Article 153.

R. Kenny Jones, Paul Guerrero, Niloy J. Mitra, and Daniel Ritchie. 2023. Shapecoder: Discovering abstractions for visual programs from unstructured primitives. *ACM Transactions on Graphics (TOG)* 42, 4 (2023), 1–17.

R. Kenny Jones, Renhao Zhang, Aditya Ganeshan, and Daniel Ritchie. 2024. Learning to Edit Visual Programs with Self-Supervision. In *Advances in Neural Information Processing Systems*.

Kacper Kania, Maciej Zieba, and Tomasz Kajdanowicz. 2020. UCSG-NET-unsupervised discovering of constructive solid geometry tree. *Advances in neural information processing systems* 33 (2020), 8776–8786.

Diederik P. Kingma and Jimmy Ba. 2014. Adam: A Method for Stochastic Optimization. *CoRR* abs/1412.6980 (2014).

Arno Knapitsch, Jaesik Park, Qian-Yi Zhou, and Vladlen Koltun. 2017. Tanks and Temples: Benchmarking Large-Scale Scene Reconstruction. *ACM Transactions on Graphics* 36, 4 (2017).

Uday Kusupati, Mathieu Gaillard, Jean-Marc Thiery, and Adrien Kaiser. 2024. Semantic Shape Editing with Parametric Implicit Templates. In *ACM SIGGRAPH 2024 Conference Papers* (Denver, CO, USA) (SIGGRAPH ’24). Association for Computing Machinery, New York, NY, USA, Article 108, 11 pages. <https://doi.org/10.1145/3641519.3657421>

Jae Joong Lee, Bosheng Li, and Bedrich Benes. 2023. Latent L-systems: Transformer-based tree generator. *ACM Transactions on Graphics* 43, 1 (2023), 1–16.

Jun Li, Kai Xu, Siddhartha Chaudhuri, Ersin Yumer, Hao Zhang, and Leonidas Guibas. 2017. GRASS: Generative recursive autoencoders for shape structures. *ACM Transactions on Graphics (TOG)* 36, 4 (2017), 52.

Gabrielle Littlefair, Niladri Shekhar Dutt, and Niloy J. Mitra. 2025. FlairGPT: Repurposing LLMs for Interior Designs. *arXiv preprint arXiv:2501.04648* (2025).

Kaichun Mo, Paul Guerrero, Li Yi, Hao Su, Peter Wonka, Niloy Mitra, and Leonidas Guibas. 2019a. StructureNet: Hierarchical Graph Networks for 3D Shape Generation. In *SIGGRAPH Asia*.

Kaichun Mo, Shilin Zhu, Angel X. Chang, Li Yi, Subarna Tripathi, Leonidas J. Guibas, and Hao Su. 2019b. PartNet: A Large-Scale Benchmark for Fine-Grained and Hierarchical Part-Level 3D Object Understanding. In *The IEEE Conference on Computer Vision and Pattern Recognition (CVPR)*.

Pascal Müller, Peter Wonka, Simon Haegler, Andreas Ulmer, and Luc Van Gool. 2006. Procedural modeling of buildings. In *ACM SIGGRAPH 2006 Papers*. 614–623.

Adam Paszke, Sam Gross, Soumith Chintala, Gregory Chanan, Edward Yang, Zachary DeVito, Zeming Lin, Alban Desmaison, Luca Antiga, and Adam Lerer. 2017. Automatic differentiation in PyTorch. (2017).

Ofek Pearl, Itai Lang, Yuhua Hu, Raymond A. Yeh, and Rana Hanocka. 2022. GeoCode: Interpretable Shape Programs. *arXiv:2212.11715 [cs.GR]*

Charles Ruizhongtai Qi, Li Yi, Hao Su, and Leonidas J. Guibas. 2017. Pointnet++: Deep hierarchical feature learning on point sets in a metric space. In *Advances in neural information processing systems*. 5099–5108.

Alexander Raistrick, Lahav Lipson, Zeyu Ma, Lingjie Mei, Mingzhe Wang, Yiming Zuo, Karhan Kayan, Hongyu Wen, Beining Han, Yihan Wang, Alejandro Newell, Hei Law, Ankit Goyal, Kaiyu Yang, and Jia Deng. 2023. Infinite Photorealistic Worlds Using Procedural Generation. In *Proceedings of the IEEE/CVF Conference on Computer Vision and Pattern Recognition*. 12630–12641.

Alexander Raistrick, Lingjie Mei, Karhan Kayan, David Yan, Yiming Zuo, Beining Han, Hongyu Wen, Meenal Parakh, Stamatis Alexandropoulos, Lahav Lipson, Zeyu Ma, and Jia Deng. 2024. Infinigen Indoors: Photorealistic Indoor Scenes using Procedural Generation. In *Proceedings of the IEEE/CVF Conference on Computer Vision and Pattern Recognition (CVPR)*. 21783–21794.

Daxuan Ren, Jianmin Zheng, Jianfei Cai, Jiatong Li, Haiyong Jiang, Zhongang Cai, Junzhi Zhang, Liang Pan, Mingyuan Zhang, Haiyu Zhao, et al. 2021. Csg-stump: A learning friendly csg-like representation for interpretable shape parsing. In *Proceedings of the IEEE/CVF international conference on computer vision*. 12478–12487.

Foundation AI Team Roblox. 2025. Cube: A Roblox View of 3D Intelligence. *arXiv preprint arXiv:2503.15475* (2025).

Gopal Sharma, Rishabh Goyal, Difan Liu, Evangelos Kalogerakis, and Subhransu Maji. 2018. CSGNet: Neural Shape Parser for Constructive Solid Geometry. In *IEEE Conference on Computer Vision and Pattern Recognition (CVPR)*.

Olga Sorkine and Marc Alexa. 2007. As-Rigid-As-Possible Surface Modeling. In *Proceedings of EUROGRAPHICS/ACM SIGGRAPH Symposium on Geometry Processing*. 109–116.

Chunyi Sun, Junlin Han, Weijian Deng, Xinlong Wang, Zishan Qin, and Stephen Gould. 2023. 3d-gpt: Procedural 3d modeling with large language models. *arXiv preprint arXiv:2310.12945* (2023).

Hou In Ivan Tam, Hou In Derek Pun, Austin T Wang, Angel X Chang, and Manolis Savva. 2024. SceneMotifCoder: Example-driven visual program learning for generating 3D object arrangements. *arXiv preprint arXiv:2408.02211* (2024).

Ashish Vaswani, Noam Shazeer, Niki Parmar, Jakob Uszkoreit, Llion Jones, Aidan N Gomez, Łukasz Kaiser, and Illia Polosukhin. 2017. Attention is All you Need. In *Advances in Neural Information Processing Systems*, I. Guyon, U. Von Luxburg, S. Bengio, H. Wallach, R. Fergus, S. Vishwanathan, and R. Garnett (Eds.), Vol. 30. Curran Associates, Inc. https://proceedings.neurips.cc/paper_files/paper/2017/file/3f5ee243547dee91fb0d53c1c4a845aa-Paper.pdf

Karl D. D. Willis, Yewen Pu, Jieliang Luo, Hang Chu, Tao Du, Joseph G. Lambourne, Armando Solar-Lezama, and Wojciech Matusik. 2020. Fusion 360 Gallery: A Dataset and Environment for Programmatic CAD Reconstruction. *arXiv preprint arXiv:2010.02392* (2020).

Peter Wonka, Michael Wimmer, François Sillion, and William Ribarsky. 2003. Instant architecture. *ACM Transactions on Graphics (TOG)* 22, 3 (2003), 669–677.

Rundi Wu, Chang Xiao, and Changxi Zheng. 2021. Deepcad: A deep generative network for computer-aided design models. In *Proceedings of the IEEE/CVF International Conference on Computer Vision*. 6772–6782.

Yue Yang, Fan-Yun Sun, Luca Weihs, Eli VanderBilt, Alvaro Herrasti, Winson Han, Jiajun Wu, Nick Haber, Ranjay Krishna, Lingjie Liu, et al. 2024. Holodeck: Language guided generation of 3d embodied ai environments. In *Proceedings of the IEEE/CVF Conference on Computer Vision and Pattern Recognition*. 16227–16237.

Yunzhi Zhang, Zizhang Li, Matt Zhou, Shangzhe Wu, and Jiajun Wu. 2024. The scene language: Representing scenes with programs, words, and embeddings. *arXiv preprint arXiv:2410.16770* (2024).

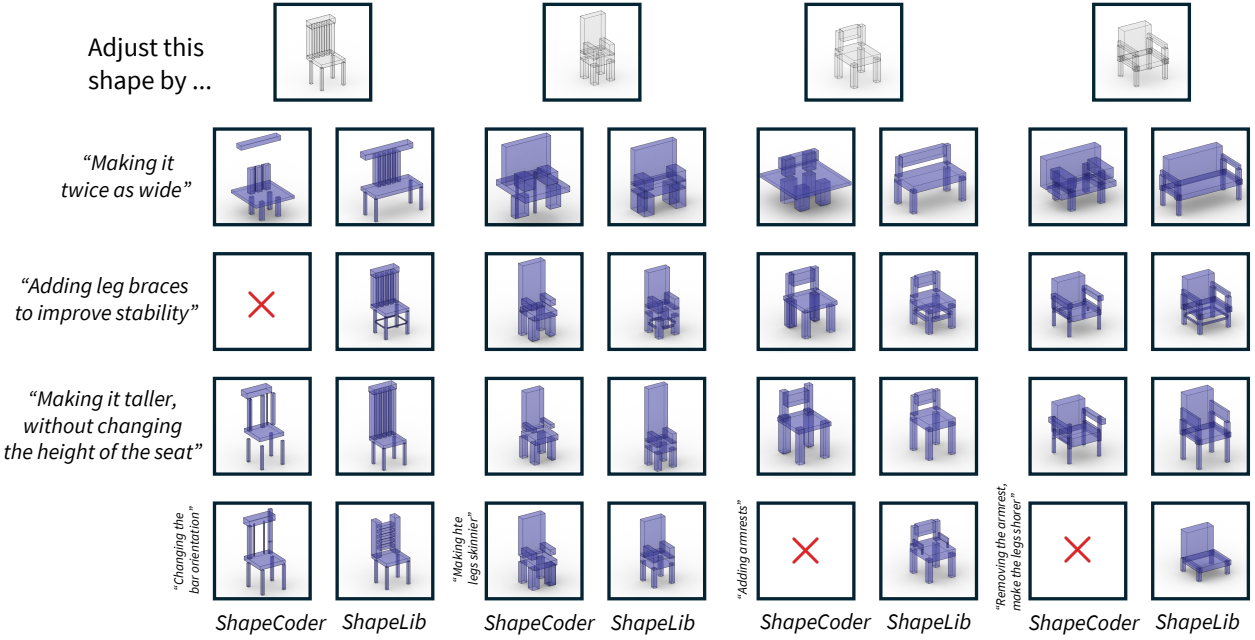
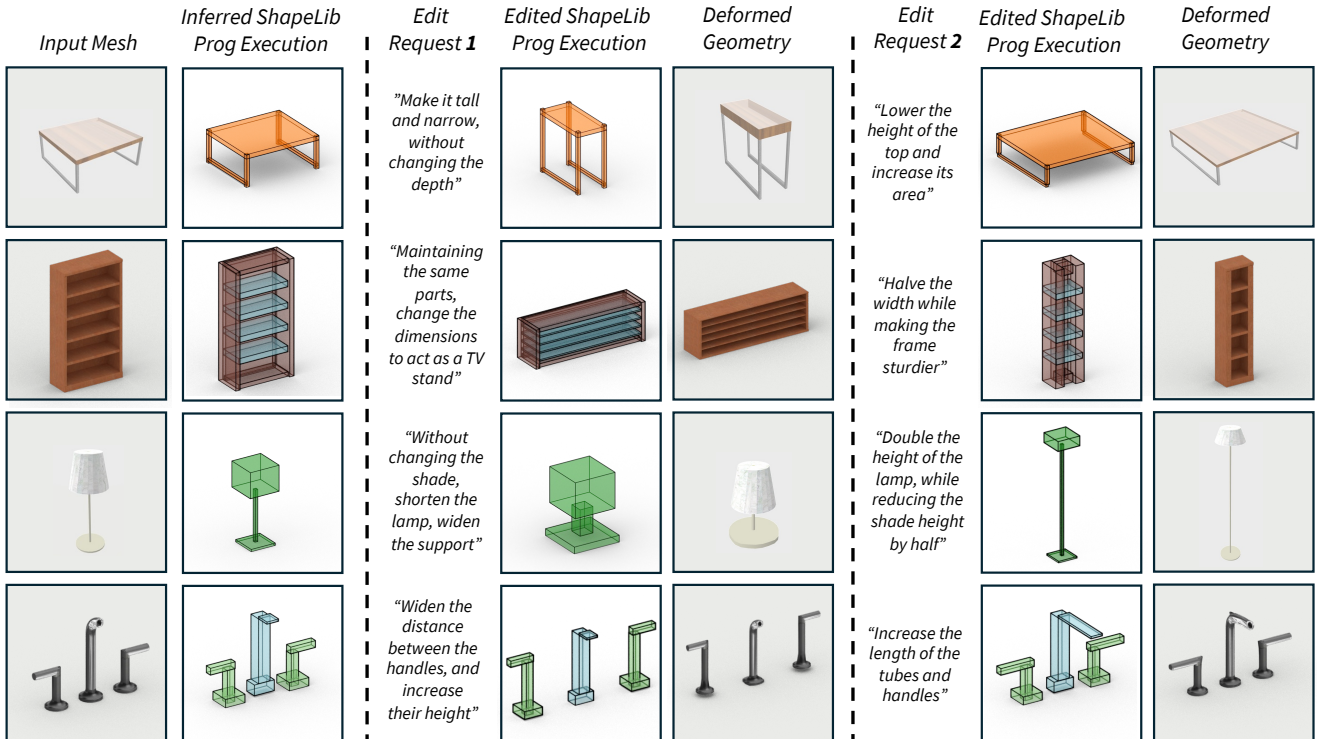
(a) LLM Shape Program Editing**(b) Structure-driven Geometry Deformation**

Fig. 5. (a): Example comparison conditions from our shape program editing study, where a LLM is tasked with editing either a ShapeLib or ShapeCoder program. LLM predictions that caused a run-time error are marked with 'X'. (b): Demonstrations of how ShapeLib can be used to edit textured meshes. Given an input mesh, we use our recognition networks to infer a ShapeLib program. This program is then edited with a LLM (we show two edit requests). This program edit then guides a cage-based deformation, using the cuboids as the cage, of the input geometry.

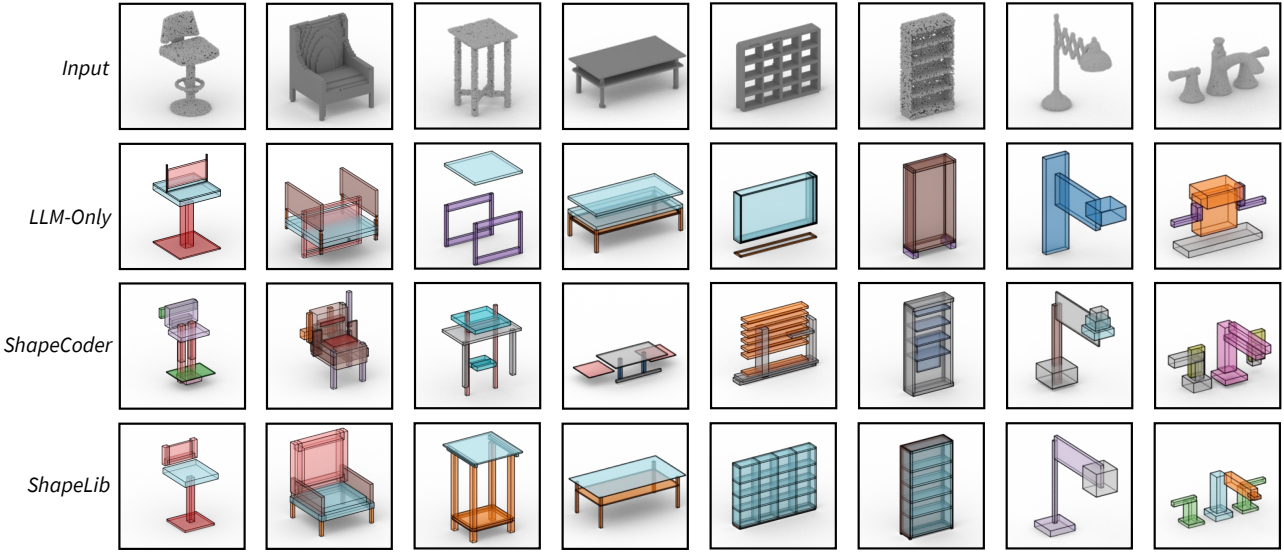
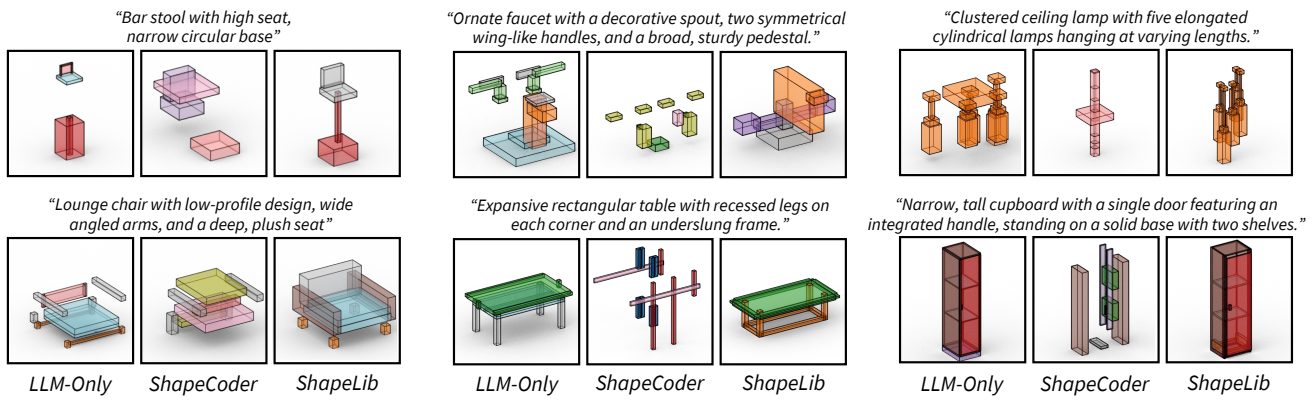
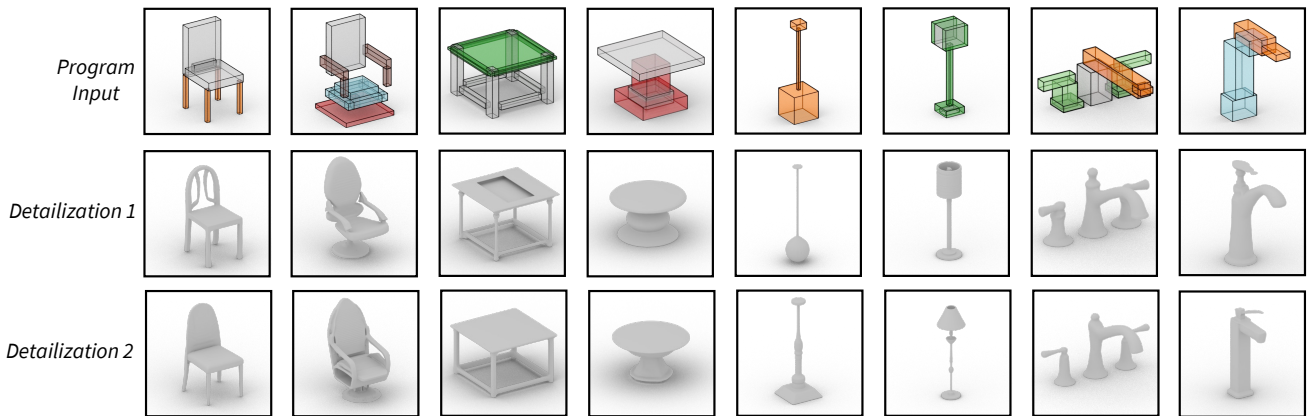
(c) Visual Program Induction**(d) Shape Program Generation****(e) Structure Conditioned Detailization**

Fig. 6. (c): Using recognition networks to convert unstructured geometry (voxels or point clouds) into shape programs. (d): Presented with different abstraction libraries, we ask a LLM to convert text prompts into shape programs. (e): We demonstrate that ShapeLib programs can be converted into detailed geometry with a structured conditioned 3D generative model, for each input program we show multiple output styles.

We describe what is included in the appendix. We provide additional results in Section A, additional method details in Section B, and additional experiment details in Section C.

A ADDITIONAL RESULTS

A.1 ShapeLib Alternative Ablations

We elaborate on the ablation experiments discussed in Section 5.4 of the main paper. Here we discuss ablations on variants of the ShapeLib method. We run experiments on the chair category, asking each method to discover libraries of abstraction functions. We report results of this experiment in Table 4, using the Function usage and the semantic consistency metrics from section 5.1 in the main paper. This involve first generating a library, then generating a program sampler from the LLM, and finally training a recognition network from this sample that conditions on a collection of cuboids and predicts a shape program that uses abstraction functions.

Below we detail the ablation conditions we consider.

LLM-Only variations. In our LLM-Only, we use *o1mini* as the LLM version, this is to match the default LLM choice for ShapeLib. One may wonder, what if another frontier LLM version could solve this problem better? We investigate this question, by replacing *o1mini* in the LLM-Only with other models, denoted in the *LLM-X* rows, under the *LLM Variants* header in Table 4. The LLM variants we consider are: *qwen 2.5 - coder* (*qwen*), *deepseek r1* (*deepseek*), and *claude 3.7* (*claude*). While some of these models do better or worse than others, none of them solve the task well, all significantly performing worse compared with the results achieved by ShapeLib. This is clear evidence that beyond just the LLM prior, it is necessary to have some geometric guidance to help constrain the libraries generation. ShapeLib uses the seed set to this purpose, overcoming some of the hallucination limitations that plague these alternatives.

Seed Set Formulation. As designed, ShapeLib takes two forms of design intent that are thought of, and provided by, a user, who has a particular modeling goal in mind. One form of this design intent is the seed set, where the user tries to pick out shapes that exhibit patterns that match the function descriptions (the other form of design intent).

How important is the selection of this seed set? To analyze how sensitive ShapeLib’s performance is to a specific seed set, we consider variants where the seed set is not chosen by the user, but rather automatically assembled. Specifically, we randomly sample shapes from a larger collection [Mo et al. 2019b] – we report two runs of such an experiment, with different random seeds, as the rows *random v1* and *random v2* in the table.

We observe that in these there is a slight drop in metric performance, but these version of ShapeLib still outperform existing alternatives (ShapeCoder or LLM-Only). We also note that using different seed sets causes some run to run variations, although the trends still remain clear. One important consideration in this setting is that common structures across the shape collection (e.g. *four leg bases*) are likely to get sampled into the seed set, while less common structures (e.g. *sled bases*) are unlikely to get added into the seed set. Without examples that match to each type of function description, not all of the functions can be validated to be correct. Case in point,

random v1 only found successful implementations for 5 out of 8 functions, while *random v2* only found successful implementations for 6 out of 8 functions. In contrast, using the user-designed seed set of ShapeLib finds successful implementations for all of the 8 described functions for the chair class.

Function Description Variations. As mentioned in the preceding paragraph, a user provides description of functions to ShapeLib as part of its inputs. These descriptions guide the LLM in how to design the interface of the library, which is how the user will interact with the functions when they have been implemented. So while the semantic meanings of these descriptions are clearly critical (e.g. what functions should be added, what types of parameters the should expose), one might also wonder how sensitive ShapeLib is to the exact format of these descriptions. To evaluate this sensitivity we ask a LLM to reword the chair set function descriptions, maintaining the semantic meaning while rephrasing each description independently. With this new set of function descriptions, we run ShapeLib, keeping the seed set fixed, these become the *LLM Reward v1* and *LLM Reward v2* rows in Table 4, under the *function descriptions* conditioning heading. Note that like in the seed set variation experiments, we report multiple runs to test sensitivity. This version shows slightly higher performance degradation compared with the seed set variation experiments, but offers performance that is still well above the baselines. We also consider a more ambitious variation, where we provide the LLM with just a function name, e.g. ladder chair back, and then ask it to produce the function description (given an in context example from another category). We call this version *LLM Generate*. While the *Prog Dof* metric is dramatically hurt (because the LLM does not design the interfaces to try to minimize exposed degrees of freedom), this variant actually achieves the best performance on the *Fns per Shape* metric, and has competitive semantic consistency performance.

A.2 ShapeLib Library Design Ablations

We ablate different parts of the pipeline involved in designing the library of abstraction functions in Table 5. In this experiment, we use the chair category, and modify different hyper-parameters of the method. K_A is number of input-output applications proposed per shape. K_I is number of proposed implementations per function. *EPS* modifies whether we consider the expanded parameter set (see Section B.1.4) or just the LLM produced input-output pairs. *ICE* modifies how the in context input-output examples are formulated for the LLM implementation stage. By default, we mask parameters with ‘?’ values (*param mask*). We consider alternatives when no input-output examples are provided (*none*) or where all input-output examples have the LLM predicted parameters not masked out (*full params*). We also consider a variant where we change the LLM model used for the function implementation proposal step, from *o1mini* to *gpt4o*.

Under variations of these parameters, we discover shape program abstraction libraries. We then record how well these libraries can represent the seed set shapes. These metrics are: the objective value (*Obj*) achieved by the resulting programs, where the goal is to have a low compression-based objective (see Section B.1.6); the number of successfully validated function applications made per shape (*Valid*

Table 4. Ablation experiment comparing alternative formulations against ShapeLib on library learning metrics. For the chair class, we report how functions are used on validation set shape, and how semantically aligned their applications are.

Condition	Method	Fn Usage		Semantics		
		# Fns per Shape ↓	Prog Dof ↓	Precision ↑	Recall ↑	F1 score ↑
<i>Baseline</i>	ShapeCoder	15.2	57.8	28	34	31
<i>LLM Variants</i>	LLMO-o1mini	14.6	65.6	51	25	33
	LLMO-claude	13.5	62.5	50	26	34
	LLMO-deepseek	13.4	61.4	54	29	38
	LLMO-qwen	17.2	74.2	43	12	19
<i>Seed Set</i>	Random v1	12.1	57.4	59	37	46
	Random v2	11.2	54.9	62	37	47
<i>Function descriptions</i>	LLM Reward v1	11.1	59.0	64	36	46
	LLM Reward v2	11.5	58.6	57	27	37
	LLM Generate	10.8	67.8	55	32	41
<i>Ours</i>	ShapeLib	10.9	53.8	65	39	49

Table 5. Ablation experiment on parameters used in ShapeLib’s library learning procedure. For chair category, we report how well the libraries represent shapes in the seed set. ShapeLib default settings, in the bottom row, outperform alternative parameter settings, justifying our design decisions.

K_A	K_I	EPS	ICE	Impl LLM	Obj ↓	Valid Fn Apps per Shape ↑	Uncovered Parts per Shape ↓
1	1	✓	param mask	<i>o1mini</i>	48.5	1.7	4.1
1	4	✓	param mask	<i>o1mini</i>	47.1	1.9	3.6
5	1	✓	param mask	<i>o1mini</i>	41.9	2.0	2.6
5	4	x	param mask	<i>o1mini</i>	44.0	2.0	3.0
5	4	✓	none	<i>o1mini</i>	45.1	2.0	3.2
5	4	✓	full params	<i>o1mini</i>	43.6	2.0	3.0
5	4	✓	param mask	<i>gpt4o</i>	43.6	2.1	2.9
5	4	✓	param mask	<i>o1mini</i>	40.7	2.2	2.2

Fn Apps per Shape) – it is good when this metric is high, as it means that the LLM has produced functions that can be used frequently over the seed set; the average number of parts in each seed set that are not explained by function calls (*Uncovered Parts per Shape*) – we want this number to be low, so that most of the parts in each seed set shape are covered by the library logic. Our default settings, in the last row, achieves the best performance for these metrics, justifying our design decisions.

A.3 ShapeLib Recognition Network Ablations

Table 6. We compare recognition network performance on point cloud to shape program reconstruction task for the chair category, under different ways of creating the *sample_shape* function.

Method	CD ↓	F-Score ↑
<i>single sampler</i>	0.046	46.5
<i>indep sampler</i>	0.043	49.8
<i>iter sampler</i>	0.039	51.8

In ShapeLib we use a LLM generated *sample_shape* function to produce training data for our recognition network. We use an iterative error correction procedure to iterate on the design of this sampler (see Section B.3)

We justify this design choice with a small ablation. For the chairs category, we take our point cloud to shape program recognition network, and train multiple versions. In the default setting, we take the initial produce *sample_shape* function, and produce two variations with a LLM prompting workflow, training on data produced by all three functions (*iter sampler*). We consider two alternatives. One, we just take the first *sample_shape* function produced by the LLM, without iterative correction (*single sampler*). As another option, we create three independent *sample_shape* functions, by using the same prompt three times, and train on data produced by all three functions (*indep sampler*).

We report results of this experiment in Table 6. For this point cloud to shape program reconstruction task, we report chamfer distance (*CD*) and F-score [Knapitsch et al. 2017]. As can be observed, the approach we adopt with iterative error-correction outperforms the alternative formulations. Using the union of three independent *sample_shape* functions is better than using a single sampling functions, but its better to generate these extra samplers with feedback sourced from the seed set.

B ADDITIONAL METHOD DETAILS

In this section we provide additional details on the various parts of our method and implementation.

B.1 Library Design

We provide additional details on the library design logic of ShapeLib. Our prompting logic has some shared commonalities – we begin with a preamble, that tasks the LLM with acting as an expert procedural modeler, that is concerned about structured shape representations.

In our prompts, we define a few helper classes as mentioned in Section 3.1 of the main paper. The *Part* class defines an axis aligned cuboid, from six input parameters: width, height, depth, x position, y position, z position. This cuboid acts as an part proxy that abstracts out detailed geometry. The *CoordFrame* class defines a local coordinate frame bounding volume. Each abstraction function ShapeLib produces takes in a *CoordFrame* object as its first argument, which controls the extents of the parts produced by the function. Otherwise, we allow the LLM to use general python syntax. We find it useful to provide the LLM with a set of general hints for how to complete this task: these include, for example, explanations for how *Part* and *CoordFrame* objects should be used, and also explain our conventions for 3D space (width runs along the x axis, height runs along the y axis, depth runs along the z axis).

B.1.1 Interface creation. In the interface creation step we use *o1mini* as the LLM. We ask the LLM to convert each function description into a structured programmatic interface: python function, with typed, named parameters, and a structured doc-string. We provide the LLM with a few in-context expert completion examples from held out categories.

We prompt the LLM such that this interface has a particular design. Each parameter is guided to be an allowed parameter type (float, strings, Booleans, integers). Each function must return a list of *Part* objects, and must take in a first argument *CoordFrame*. In the doc-string, there are certain fields we check for. The ‘Description’ field provides an overview of how the function is expected to be implemented. The ‘Parts’ field expresses the possible structural configurations the function can produce. The ‘Parameters’ field describes what effect each input parameter has on the output part structure. Note that the ‘Parts’ field always need to include a ‘Valid options’ list, that states what numbers of parts could be created by the function. We use this ‘valid options’ list to help prune out obviously bad LLM applications in later stages. Note that each entry in ‘valid options’ must be greater than 1, as there is no compressive advantage in having an abstraction function that takes in a *CoordFrame* object and returns a single *Part* (that would have to match the extents). Note we also ensure that each ‘string’ type argument has a defined valid options list in the doc-string, so really these ‘strings’ act as lightweight Enums.

B.1.2 Propose Function Applications. In this stage, we give a shape to an LLM, along with the interface, and ask it to write a program that would reconstruct the shape. We represent the shape in a structured fashion, as a list of *Part* objects, where each part has dimensions, position and semantic label from a seed set shape. We also pass a render of the mesh to a VLM (gpt4o), asking the VLM to describe the parts that are present in the shape.

From these two inputs, the task is then to write a program that uses functions to recreate the input part list. For this purpose, we

give the LLM access to a specially designed *group_parts* functions. This *group_parts* function, takes in a list of *Part* objects, and automatically returns a *CoordFrame* bounding object. We provide the LLM with some out-of-category in-context examples that show how to perform this task for a toy library. We ask it to try to explain all parts in the shape with calls to the library functions, though if there are any single parts that cannot be explained through library calls we allow the LLM to identify these with independent *group_parts* calls.

After the LLM predicts a program, we evaluate the function applications. For each function, we look at the parts that the function is trying to explain (using the *group_parts*), and can reject bad groupings of parts that are not possible under the constraints of the ‘valid options’ part of the interface. We record triplets of function name, function parameters, and input parts (identified through the *group_parts* call).

For each shape, we perform this procedure 5 times. The first time we use *o1mini* as the LLM. The subsequent times we use *gpt4o*, as we find that even reasoning LLM modules struggle to exactly predict correct parameters, so we use the LLM to instead generate approximately correct solutions (that we later validate geometrically).

B.1.3 Proposing Function Implementation. In this step we use *o1mini* as the LLM. We provide the LLM with input-output examples, sourced from previous step, and ask it to propose a python implementation of the function. Besides the typical hints, we task the LLM with making sure that each parameter, when changed, updates the output geometry (no parameter should be a ‘no-op’). Beyond this, parts should not float in space (they should have a connected path to the ground).

When we format the input-output examples, we omit all of the parameter values with ‘?’; we ablate this design decision in Section A.1. From all of the function applications, we select a maximum of four in context examples, choosing randomly from the LLM applications, making sure to evenly sample from each shape in the seed set as much as possible.

After the LLM authors a new implementation, we hypothesize that it might find improved parameterizations of the function for the input-output examples (now that it knows how the function works). To leverage this observation, we add an additional request to the LLM: “after you have written your implementation, provide a parameterization for each input example that would recreate its associated output.” We then record these new predictions as input-output examples for the validation stage.

B.1.4 Library Validation. Library validation happens on a per function basis. For each function, we find every single group of parts that the LLM ever said could be explained by the function in question. Then we also consider all of the parameterizations the LLM ever suggested for the function. LLMs are good at generating hypothesis that are approximately correct, and we observe they perform better when the task is more tied to semantics; for instance, they do a good job at identifying which functions to use, and which parts they should explain parts, but they are not as adapt at exactly predicting continuous parameter values.

With this in mind, we would like to take the set of proposed function parameterizations, and expand it to search for more ways

that the function could be executed, which is important in order to check which of the proposed implementations have potential outputs that could validate with respect to structures in the seed set. So, for each parameter, independently, we identify all unique values observed in the function applications. For boolean and string parameters, where know the possible values ahead of time, we consider all of these values. For floats, we greedily build up a set, with a minimum gap of 0.025, where if we have already added a parameter with value a , and a new parameter comes up with value b , and the distance between a and b is less than this gap, we don't add b into this unique set. From this unique set, we then consider all of the possible combinations, doing a cartesian product over this list of lists. If the size of this product is greater than a max value (10000), then we sub-sample 10000 options from this list. We always consider the LLM predicted input-output examples first, and then augment this set with the new parameterizations. We ablate this design decision in Section A.2.

Then, for each parameter group produced from this set, we try executing each function implementation. Against every identified group of parts from the input-output examples, we compute the error between the function output and the goal layout – if this error is below a set threshold, we record a success (see next section). An implementation needs at least 2 successful validations (on separate seed set shapes) for us to include it into the library. We only include up to 1 implementation per function, so we choose the implementation that achieves the lowest error, for the most seed set shapes.

Finding programs for seed set shapes. After the validation step we have implemented functions, and we know which function applications can explain which parts in which shapes, but we don't know what is the best program to explain each shape in the seed set. We would like to optimize the objective function (see below). To accomplish this, we take a greedy approach, for each (function, parameterization, and part group) triplet that was validated, we record the objective function incurred, averaged over the number of parts the function recreates. We then sort the validated function application according to this score, and build up a program by taking the next best function application in a greedy fashion. In this step, we make sure to skip function applications that try to recreate parts that a previously used function line have already covered. Any leftover parts are represented with a special *make_part* function that just defines a *Part* that has a semantic name.

B.1.5 Primitive Error Function. The geometric error function we use takes in two sets of unordered primitives. For every pair of primitives from the predicted to target set, we calculate the maximum minimum distance between any two corners from one primitive to the other. We then use a matching algorithm to assign a stable pairing between the two sets. If any of the distances is above a threshold (0.25, where shapes are normalized to lie within the unit sphere), then we say that there is infinite geometric error. Otherwise, the geometric error is an average of the MMCD's calculated according to the best match.

B.1.6 Library Learning Objective Function. When searching for programs that explain shapes, we need an objective function to guide

the search. We take inspiration from prior approaches such as [Jones et al. 2023], and formulated an objective function as a weighted average of two terms. One of these terms counts up the number of degrees of freedom in the program representation, for simplicity we treat every token in the program as a degree of freedom with the same weight (1.). Another term ensures that the produced geometry does not deviate too far from the target structure. We calculate the geometric error (above), and add that into our objective function with a weight of 10.

B.2 Recognition Networks

We implement all of our networks in PyTorch [Paszke et al. 2017]. All of our experiments are run on NVIDIA GeForce RTX 3090 graphic cards with 24GB of VRAM. We use the Adam optimizer [Kingma and Ba 2014] with a learning rate of 1e-4, dropout of 0.1, and a batch size of 128. All of our networks train on synthetic data that is sampled ‘on-the-fly’ from the LLM authored *sample_shape* function, we use 25 million programs for structured input networks, and 16 million programs for unstructured input networks, observing that the loss curves reach saturation at this point. This training takes between 12 hours and 48 hours, depending on category and input modality.

B.2.1 Network Architecture. We implement our recognition network as a Transformer decoder. Our network has 4 layers, 4 heads, model dim of 256, and a full feature dim of 1024. This network has full attention over the conditioning information, each visual input is tokenized in a particular fashion (see below). Programs are similarly tokenized, and our network is trained through teacher forcing, because as we have paired data, we can use cross entropy loss. This is the same loss that LLMs use in pretraining, or supervised finetuning stages. We use learned positional encodings, these cap the maximum sequence lengths.

B.2.2 Structured Inputs. We describe the process for mapping a collection of cuboids to a shape program. First, each parameter in each primitive in the input shape is quantized and treated as a discrete token. We order the primitives according to their x-y-z positions, as we do not know how they should be ordered otherwise. We learn positional encoding for the positions of the input parameters, so our network can reason over up to 20 primitives and programs of up to length 64 (for structured nets) and length of 128 (for unstructured nets). For primitives, we find it useful to perturb the cuboid parameters of the input a bit, so the network does not overly pick up on ‘perfect’ patterns produced by executing the cuboids. To this end, we add a noise of gaussian level 0.05 to each cuboid parameter. Note that this changes the input to the network, but the target program does not change, this acts similar to dropout, as a kind of regularization on learning.

Inference procedure. Our inference procedure prompts the network with an input set of unordered primitives and samples a large number of programs according the network's predicted distribution. We try executing each program, and we record its complexity (the number of tokens it uses) and its geometric error against the input set (using the a geometric error metric, Section B.1.5). We sample programs independently up until a timeout (4 seconds per shape)

– note this is half the time that ShapeCoder uses on average per shape inference. We choose the program that minimizes an objective that is a simple weighted combination of these two values, see Section B.1.6.

As we know the ground truth set of primitives we are trying to get the program to recreate, we can also integrate a more advanced search strategy. Say we have one version of the program a , that has achieved the best objective value so far. Now say we predict another program version b , that achieves a worse objective value. While we could just throw the entire prediction of b away, instead we can consider all of the sub function applications made in b , and check if any of these calls, if merged into the program version a , would improve its objective function score. This more involved search strategy offers only a small, but significant improvement, and mirrors similar primitive based reconstruction approaches adopted by prior work [Jones et al. 2023].

B.2.3 Unstructured Inputs. We describe the process for mapping unstructured geometry (e.g. a point cloud or an occupancy voxel field) to a shape program. For point cloud inputs, we replace the primitive token encodings with an embedding produced by a Point-Net++ [Qi et al. 2017] network. This network produces 4 visual tokens. For voxel inputs, we replace the primitive token encodings with an embedding produced by a 3D-CNN. This network produces 8 visual tokens.

To convert a program into a point cloud, we first execute the program to produce a collection of cuboids. We convert these cuboids into a mesh (not worrying about intersections), and then sample a point cloud from the surface of the mesh (2048 points for all experiments, without normals). To convert a program into voxels, we take a set of query points (voxel centers), and evaluate the local position of these query points within each cuboid. If the query point is inside any cuboid, or the distance to the nearest cuboid is less than half the length of a voxel, we say the voxel is ‘occupied’, otherwise the voxel empty. Use voxel fields of size 64x64x64.

Inference procedure. During this inference procedure, unlike the structured visual program induction setting, we don’t know which parts should be created. So here, we just sample a large number of programs from the network: 1000 independent samples, using Top-P sampling (with P=90%). For each sampled program, we try executing it, convert the output cuboids into a point cloud, and record the reconstruction performance. We choose point cloud reconstructions based on the Chamfer distance between the input and sampled mesh. We choose voxel reconstructions based on the IoU between input voxel and output voxel field. F-score [Knapitsch et al. 2017] is another metric we consider for point cloud reconstructions, using a threshold of 0.03 (where meshes are normalized to lay within unit bounding box).

B.3 Synthetic Data Sampler

We task the LLM, provided with the interface and validated seed set programs, to author a *sample_shape* function. We tell it that this function should randomly produce new procedural shapes using the library of functions, that the sample shape function should take

in a single *CoordFrame* parameter, that specifies the global bounding volume of the shape to be produced.

We use LLM models with reasoning capabilities (e.g. o1), as this task is quite difficult, to author a convincing data sampler. After the LLM authors a version, we see how well it actually matches the patterns in the seed set. We perform two rounds of automated feedback for each function in the dataset. In each round of feedback, we evaluate the function by sampling a diverse set of shapes and assessing various aspects of its behavior. We examine whether all functions in the library were used, whether all parameter types were employed, and whether all output structures described in the function’s documentation were produced. These checks are performed automatically. Additionally, we analyze the structures generated by the sampled function applications to determine their similarity to those observed during the validation stage. If any significant deviations are detected, the sampler is instructed to update its logic to produce outputs closer to the expected structures. The goal of this procedure is not necessarily to produce a ‘better’ sample shape function, but rather to produce variations that explore different parts of the seed set space. During training of recognition networks we randomly sample from all LLM produced sample shape functions; we randomly choose a sampling function, then randomly sample a program, to see a more diverse spread of programs. See Section A.3 for an experimental ablation on this design decision.

B.4 Generation and Editing Applications

B.4.1 Detailization. We develop a detailization module, that can convert a layout of cuboids to a 3D mesh with geometric details. We take a pretrained text-to-3D shape generative model, Cube [Roblox 2025], and adapt it to instead condition on a layout of primitives (not text). We first describe the base Cube model, and then describe our adaptation.

Base Cube Model. The base cube model is composed of two parts. One part of the system is an encoder-decoder, the encoder takes in a point cloud and outputs a sequences of discrete codes (512 in length). The decoder takes this sequence of discrete codes, and uses marching cubes to produce a 3D mesh, after predicting per-point occupancy values. We do not change the encoder or decoder part of the pipeline, keeping them frozen. Then a decoder only transformer module learns to model sequences of these discrete codes in an autoregressive fashion. Given an input shape with an accompanying text prompt, they embed text prompt into a set of 77 tokens using a frozen clip encoder. The transformer attends over these 77 tokens, and autoregressively predicts next 512 shape tokens one at a time, which can then be converted into a 3D mesh with the decoder.

Structured adaptation. In our adaptation, we start with the pre-trained, released model. We remove the CLIP conditioning, instead we add in a box encoder. This box encoder consumes a layout of cuboid primitives, lifts each primitive to a higher dimension with a linear layer, and then we use attention layers to blend this feature space together. This process produces up to 20 new tokens, which the transformer attends over. We finetune the attention weights

of the transformer, and all parameters of the box encoder, while keeping all of the feed forward layer weights frozen.

We finetune this network with paired cuboid layouts and meshes with geometric details; sourcing this data from PartNet [Mo et al. 2019b], training in a per-category fashion. We normalize the cuboid layout, so that the entire layout is centered and has extents that match the unit sphere. After decoding a mesh, we then transform the output shape to match the original dimensions of the input layout. To formulate training data, for each input mesh, we sample the surface to produce a point cloud, and then encode this point cloud into a sequence of discrete codes using the frozen encoder. We then condition the network on the features produced by the box encoder, and update the network with cross entropy loss, using teacher forcing, on the *GT* sequence of discrete codes. We train on between 1000 and 6000 shapes per category, which takes between 2-4 days until loss convergence, with a batch size of 4, a learning rate of 1e-5, with 24GB of ram.

To integrate this network with ShapeLib programs, we take programs, execute them to get a layout of cuboids, feed this layout into the network, and get out a sequence of discrete codes. This sequence of discrete codes can be presented to the frozen decoder to produce a 3D mesh. We sample from the transformer without classifier free guidance, with Top-P sampling of 90%, so we get variations in the style, and quality, of the detailizations. In future work, it would be interesting to try to automatically identify which samples have a better (or worse) adherence to the input part layout conditioning. We visualize some of the detailizations in Figure 6 (e) of the main paper.

B.4.2 Structured Deformation. In Figure 5 (b) of the main paper, we demonstrate that ShapeLib program edits can drive mesh edits through a deformation scheme. We use a simple deformation scheme inspired by cage-based deformation schemes. Assume we have: a starting mesh, with vertices and faces; a starting cuboid layout, produced by program version 1; an edited cuboid layout, produced by program version 2. Critically, we assume this layout change was made by a program edit, so we know the correspondence between the cuboids in the starting layout and the cuboids in the edited layout.

With this input, our scheme operates as follows. For each mesh vertex, find the local position of the vertex within each cuboid in the starting layout. Then assign a weight of this vertex to each cuboid. How do we assign this weight? If the vertex is inside a single cuboid, all of its weight goes to that cuboid. Otherwise, if the vertex is inside multiple cuboids, or no cuboids, we assign the weight as distribution over all of the cuboids. This distribution is determined according to a soft blend, that uses the inverse of the distance of each point to the surface of each cuboid to determine the shape of the distribution.

With this weighting scheme, given a new primitive layout, we can produce new vertex positions. We calculate the local position of each vertex with respect to each new cuboid placement, and then average these positions with respect to the cuboid weighting distribution. Note, that in this scheme, the face structure of the mesh does not change.

Our formulation does not currently support removing or adding parts, so we assume that program edits change only positions and

or the dimensions of the cuboids. This editing scheme could be replaced with other, more sophisticated solutions ([Kusupati et al. 2024]), or be improved by adding in regularization terms ([Sorkine and Alexa 2007]) but as demonstrated in Figure 5 (b) of the main paper, this simple approach already works well enough to produce compelling sets of edits.

C ADDITIONAL EXPERIMENT DETAILS

In this section we provide additional details on our experimental design. As an overarching note, we point out that in the figures of all rendered program executions, we maintain a consistent color for the cuboids created by a certain function; e.g. every cuboid created by a 'ladder chair back' call is given a green color (see Figure 2, in main paper). When cuboids are created without a semantic abstraction (e.g. a Part is directly instantiated) we color the output parts in gray.

C.1 Cost and Timing

We provide detailed estimates for how expensive it is (from a time and API monetary expense perspective) to use our system to discover libraries of shape abstraction functions. To produce 20 shape descriptions from images using *gpt4o*: 10 cents and 1-2 minutes. To create library interfaces from textual descriptions with *o1mini*: 25 cents, 2-4 minutes. To propose function applications over (20) shapes with (1) *o1mini* call and (4) *gpt4o* calls: \$2-3 and 15-25 minutes. To propose (4) implementations for each function with *o1mini*: \$2-4 and 15-30 minutes. To propose a single program sampler with *o1*: 50 cents and 1 minute. Validation takes between 5 and 20 minutes per category, depending on the number of functions and the size of the parameter sets to evaluate.

C.2 Data

Collections of example shapes in the seed set are chosen by an user, with the idea that they should match the design intent expressed in the function descriptions. The design of the function descriptions was done up-front, without iteration, where a expert expressed domain knowledge to the LLM in a easily transmissible medium. See Section A.1 where we ablate this user input. Specifically, we have the user select 20 partNet shapes and put them in a list, and then we can automatically produce the rest of the structured data from the partNet annotations. Shapenet meshes with texture are then rendered, using metadata in partNet.

After creating seed sets, we created validation sets of held out PartNet shapes: chairs (1000), storage(400), tables (1000), faucet (400), lamps (656). All experimental results in the main paper are done on the validation shapes, never seen before by ShapeLib.

C.3 ShapeCoder

Library Generation. ShapeCoder is the best existing method for library learning over 3D shapes. ShapeCoder tries to discover abstraction functions that improve a compression-based objective over a dataset. In our comparisons against ShapeCoder we use the officially released implementation, and run it over the seed sets. The only change we make is removing the rotation operation from the base ShapeCoder language, as we focus on structures of axis-aligned primitives in our experiments.

Recognition Network Training. ShapeLib uses a LLM produced sample shape function to get training data for its recognition network. ShapeCoder takes a different approach, sampling random parameterizations of functions, and then creating synthetic data by randomly combining these functions into random scenes. This scheme was originally proposed *only* to train recognition networks (with a related architecture) that map cuboids to shapeCoder programs. For our structured reconstruction tasks (function usage and semantic consistency in Table 1, main paper) we use these networks. To allow ShapeCoder to perform unstructured visual program induction tasks (mapping point clouds or voxels to shape programs), we adapt this framework, by taking our recognition networks and training them to predict ShapeCoder programs. For these networks, we follow the original ShapeCoder formulation using random combinations of functions as scenes, as ShapeCoder cannot leverage the prior from a LLM to produce sample shape function.

LLM Usage Experiments. We experiment with how well LLMs can interact with ShapeCoder programs, and find that this is challenging for frontier models. ShapeCoder functions and parameters do not have semantic-aligned names, and tend to over-focus on local patterns, especially when discovered on small seed sets. To try to help the LLM as much as possible, we provide prompts where each abstraction is presented with its definitions, along with an expert documented base ShapeCoder library.

C.4 LLM-Only

Library Generation. LLM-Only is an ablated version of our method that relies on only the prior of the LLM and the design intent of the expert user in the form of function descriptions. We compare ShapeLib against this condition to validate the need for using the seed set of shapes alongside the natural language specification. By default we use *o1mini* as the LLM for this condition, but experiment with other LLM versions in Section A.1.

This baseline is equivalent to ShapeLib modulo a few critical changes. The interface creation step is exactly the same. After this step though, LLM-Only immediately implements each function, without using any input/output guidance about how this function should be constructed. As it has no seed set, it assumes that the LLM has perfectly implemented each function, and cannot validate whether its production was ‘good’, or just a hallucination.

Recognition Network Training. After the LLM has produced a library of shape abstraction functions, it next advances to the synthetic sampler design stage where it prompts the LLM to produce a *sample_shape* function. However, as LLM-Only doesn’t have access to a seed set, it cannot source in-context examples of how functions can be used to represent seed set shapes. This also means that the *sample_shape* function cannot be improved with our iterative error-correction approach. Then, like the full ShapeLib system, we can train a recognition network on data produced by randomly sampling this procedure.

LLM Usage Experiments. Like ShapeLib, LLM-Only has a function library that exposes an interpretable programmatic interface. At the same time, its functions don’t produce outputs that are as useful in

representing ‘real’ shape geometries, as we’ve demonstrated extensively. In terms of how this impacts LLM interaction, as LLM-Only doesn’t have access to the seed set, for various tasks (like the text-to-shape prog generation), the baseline does not get in-context examples of text and program paired data, whereas ShapeCoder and ShapeLib can use the seed set to source this information.

C.5 LLM Shape Editing

In Section 5.2 of the main paper, we presented a LLM editing experiment. Here, we provide additional details on the design of this experiment. We sourced 5 shape programs from the validation set of each category, and consider 4 edits per shape, giving us a cross-product of 100 total comparison conditions. We use *o1mini* as the LLM, and observe that *o1mini* produced ShapeCoder programs that had a failed execution for 11/100 conditions (so we omit those from the study). Note, that none of the edited ShapeLib programs had execution errors.

We recruited 13 university students to perform the perceptual study. Each participant made 25 judgments on two questions for each shown comparison. Question 1: “Which edited shape better matches the intent of the request?”. Question 2: “Which edited shape has a more plausible structure?”

C.6 LLM Shape Program Generation

We are interested in measuring the usability of the libraries of programmatic shape abstraction functions discovered by different methods. To this end, we designed a LLM shape program generation experiment, see Section 5.3 of the main paper. We wanted to see if an LLM (taking the place of a user interacting with shape programs) could use the library to create reasonable novel shape structures. To get diversity in the outputs of the LLM, we give it a text description of some shape that the program should exemplify. Note, that we do not directly measure how well the output structure adheres to the input prompt, but rather we use the set of text prompts to generate a diverse set of structures. We can then measure how close this set of structures is to a set of GT shape structures sourced from validation shapes of the same category. That said, as evidenced by the qualitative results in Figure 5 (d) of the main paper, beyond producing more plausible shapes, ShapeLib also does a solid job of adhering to the semantic request of the input – though we found it difficult to directly measure this property.

How do we generate the set of prompts in this experiment? For each category, a user annotates simple descriptions of 10 seed set shapes. Then we use these as a seed for LLM ideation, asking the LLM, iteratively, to take these text prompts as a starting point and come up with new descriptions in the same style. We repeat this 10 times, producing 5 new descriptions each prompt, to get 50 total text descriptions per category.